Charge-coupled devices combined with centroid algorithm for laser beam deviation measurements compared to position sensitive device

Bo Hou, Zong Yan Wu, Jean-Louis de Bougrenet de La Tocnaye, Philippe Grosso

Charge-coupled devices combined with centroid algorithm for laser beam deviation measurements compared to position sensitive device

Q1 **Bo Hou**
Z. Y. Wu
J. L. de Bougrenet de la Tocnaye
P. Grosso
Telecom Bretagne
Optics Department
Technopôle Iroise 29238
Brest, France
E-mail: bo.hou@telecom-bretagne.eu

Abstract. A position sensitive device (PSD) is frequently used in laser beam deviation measurement. However, it lacks the capability to retrieve the power distribution information of a laser beam. A charge-coupled device (CCD) gives much more information of a laser beam than a PSD. The requirement of a multifunctional sensor makes the replacement of a PSD with a CCD in measuring laser beam deviation to be a reasonable topic. In this paper a performance comparison between a PSD and a CCD combined with a centroid algorithm are discussed with special attention paid to the CCD-based system. According to the operating principle of the CCD-based system, several experiments were carried out to evaluate five factors of the CCD-based system: image window size, number of processed images, threshold, binning, and saturation. By applying the optimized parameters, several experiments were made to compare the CCD-based system with the state-of-the-art PSD-based system in terms of two performance indicators, namely resolution and speed. It is shown that, by applying the optimized parameters, the performance of a CCD-based system is comparable to that of a PSD-based system in measuring laser beam deviation. [DOI: 10.1117/1.3554379]

Subject terms: charge-coupled device; position sensitive device; centroid algorithm; beam deviation measurement.

Paper 100548RR received Jul. 8, 2010; revised manuscript received Jan. 6, 2011; accepted for publication Jan. 19, 2011; published online Mar. 00, 000.

1 Introduction

Since laser technology has been developed for years, it has been widely used in different applications, one of which is to measure physical parameters by detecting the laser beam deviation.[1,2] In this framework, a position sensitive detector (PSD) is an optical sensor that can measure a light spot location in one or two dimensions on a sensor surface. In 1957, Wallmark[3] first introduced the lateral-effect photodiode PSD which has been extensively developed, including in performance analysis,[4] signal processing methods,[5,6] and various applications. As an analogue device, a PSD provides high sensitivity, short response time and independence from spot light size, shape and intensity. Due to these features, a PSD has been used for various laser beam deviation measurement systems. However, the PSD analogue output signal makes it hard to benefit from modern post-processing techniques. In 1969, the charge-coupled device (CCD) was invented by Boyle and Smith, recording illumination in a pixel-based image. With the development of image post-processing techniques, the CCD becomes a way to measure laser spot deviations. Compared to analogue PSD, the pixel-based CCD does not directly provide information on position, but rather on laser spot shape and intensity. The position information can then be retrieved by different post-processing algorithms. This feature makes the pixel-based image sensor extremely flexible for laser beam deviation detection, with more capacity to extract additional useful information. Our previous work involved developing a refractometer to measure the salinity of seawater based on measuring the laser beam deviation with a one-dimensional(1D) PSD.[7] The resolution of measuring salinity reaches 0.002 g/kg with the measurement range from 0 to 40 g/kg. Besides the salinity, other quantities of seawater, for example, the turbidity, are very important for the oceanology. This information, which is highly associated with the power distribution of laser spot, cannot be retrieved from neither 1D PSD nor two-dimensional(2D) PSD, for example, the quadrant photodiode.[8] Because of this, the CCD, which is sensitive to the power distribution of light, is considered to be a replacement of the PSD. To achieve this, it is necessary to have a performance comparison between a CCD-based system and a PSD-based system, and prove that a CCD-based system could at least obtain the same resolution in laser beam deviation measurement.

To retrieve the position information from the images captured by a CCD, a localization method is needed to be applied to the images. Several previous researches involved different localization algorithms. Canabal et al.[2] compared three localization algorithms: centroid, Gaussian fitting, and Fourier transform. Welch[9] worked on the effects of the window size and the shape on the centroid algorithm. Bobroff's article[10] describes the theoretical limits on the ability to locate a signal position. The comparison between a quadrant diode-based system and a CMOS-based system was studied by Scott et al.[8] Other researches on the CCD-based laser beam deviation measurement has focused on the comparison among several post-processing techniques[11] and estimated those algorithm accuracies,[12,13] including system error and

noise, to improve accuracy.[14–17] Because a PSD actually gives the gravity center of a laser spot, in this paper, the centroid algorithm, which is also calculating the gravity center, is combined with a CCD to compare with the state-of-the-art PSD-based system.

A 1D-PSD transfers the laser beam illumination into two photocurrents, which implies the position of the laser beam. This limits the post-processing methods of the PSD-based system, although it provides a very fast speed. Another drawback of PSD-based systems is that the high resolution of such systems relies on the assumption that the two analogue photocurrents should be amplified with two identical amplifiers, which is difficult to be achieved at a low cost. On the other hand, the CCD stores the intensity of the laser beam into an array of pixels. Many smart post-processing algorithms can then be applied to compute the laser beam position, including centroid, squared-centroid, fitting, Fourier, edge detection, etc. One of the issues with the CCD-based system is its low speed, caused not only by the longer hardware response time, but also the post-processing algorithm complexity. However, the flexibility of CCD-based systems provides greater freedom to balance performance (e.g., the image window size, laser beam intensity, and threshold, etc.).

This paper first compares the principles of both methods. Based on these principles, two key performance indicators, resolution and speed, are analyzed with particular attention paid to the issue of sensor saturation, which is a key feature that may result in unexpected errors, as illustrated at the end of Sec. 3. During the discussion, various performance improvements are proposed for both systems. According to these improvements, experiments have been performed to assess the performance with different parameters compared to the state-of-the-art PSD-based system. Experimental results and analysis are presented in Secs. 5 and 6.

2 Principle

2.1 *PSD-Based Laser Beam Displacement Measurement*

The principle of a 1D PSD is shown in Fig. 1(a). The PSD has a single active area formed by a P-N junction. The two parts that originated from the laser spot to the two electrodes form two lateral resistances for the photocurrents running toward the electrodes. The photocurrents are collected through the resistances by the output electrodes, which are inversely proportional to the distance between the electrode and the center of the incoming light beam. This relationship is expressed as follows:[18]

$$x = \frac{L}{2}\frac{I_2 - I_1}{I_2 + I_1}, \tag{1}$$

where I_1 and I_2 are the electrode photocurrents, L is the length of the PSD active area and x stands for the laser spot position. According to the principle, the center given by a 1D PSD is the gravity center of incident light. The post-processing process, which is typically implemented by the external processing circuit, first amplifies each of the photocurrents, transfers them into voltages, and then calculates the subtraction, addition, and division operations in Eq. (1).

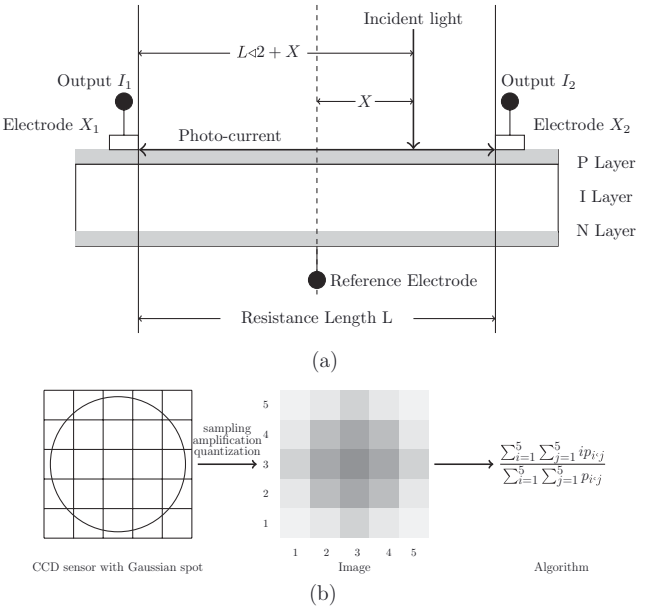

Fig. 1 The operating principles of both 1D PSD and CCD. (a) The operating principle of 1D PSD. (b) The operating principle of CCD-based system, a Gaussian beam (shown as the circle) shoot on a 5×5 pixels CCD. After sampling, amplification and quantization, the image records the power distribution of the Gaussian spot. An algorithm is then utilized to retrieve the position of the spot from the image.

2.2 *CCD-Based Laser Beam Displacement Measurement*

Figure 1(b) shows the operating principle of a CCD-based system. The image-capture process of a CCD-based system contains sampling, amplification, and quantization. It first samples the optical intensity and then converts the sample into a signal charge, which is transformed into voltage through a common output. After voltage quantization, all signals are processed by the post-processing algorithm to calculate the position. As mentioned in Sec. 1, many algorithms can be used for laser beam position calculation. Algorithm selection is based on the definition of the laser beam position, which highly depends on the applications. To compare with a PSD, the definition of the laser beam position should be defined as the same as the PSD-based system, which is the gravity center of the laser spot. Therefore, the centroid algorithm has been used here to calculate the gravity center due to its simplicity.

To analyze the resolution of the CCD-based system, a laser beam distribution model should first be introduced. A Gaussian beam is commonly used as a laser intensity model. A Gaussian beam $g(x, y)$ with peak intensity I_0 and beam waist r_0 is expressed as:

$$g(x, y) = I_0 e^{-x^2+y^2/2r_0^2}. \tag{2}$$

After sampling by the pixels of the CCD, we can get the sampled signal:

$$p(x, y) = g(x, y)s(x, y) = \sum_{j_1=-\infty}^{\infty}\sum_{j_2=-\infty}^{\infty} g(j_1\Delta x, j_2\Delta y)\sigma(x - j_1\Delta x, y - j_2\Delta y), \tag{3}$$

where $p(x, y)$ is the sampled signal, and $s(x, y)$ is the sampling function. Here σ stands for the dirac function. After

sampling, the signal is quantized using different methods. To simplify, we leave this point aside in this paper. According to the centroid algorithm, the 1D center of the laser spot could be expressed as:

$$x = \frac{\sum_{i=-\infty}^{\infty}\sum_{j=-\infty}^{\infty} ip_{i,j}}{\sum_{i=-\infty}^{\infty}\sum_{j=-\infty}^{\infty} p_{i,j}}. \tag{4}$$

From Eq. (3), the sums in Eq. (4) can then be replaced by the integral, and the centroid of the function $p(x, y)$ can be represented as follows:

$$x = \frac{\int_{i=-\infty}^{\infty}\int_{j=-\infty}^{\infty} ip(x, y)dxdy}{\int_{i=-\infty}^{\infty}\int_{j=-\infty}^{\infty} p(x, y)dxdy}, \tag{5}$$

which results in the following formula by Fourier transformation:[19]

$$x = -\frac{P_u'(0, 0)}{2\pi j P(0, 0)}, \tag{6}$$

where $P_u(x, y)$ is the Fourier transform of $p(x, y)$, and $P_u'(x, y)$ is the derivative of P_u.

3 Performance Analysis

3.1 *Resolution*

The resolution of a CCD-based laser beam deviation measurement system depends on three aspects: systematic error caused by sampling, quantization and centroid algorithm, systematic error due to noise, and their corresponding uncertainties. We assume here that the laser spot moves a distance d from position X_0 to position X_d along the x axis. Let e_c be the systematic error caused by the sampling, quantization, and centroid method. The following relationship exists:

$$x_d = \bar{x}_0 + d + e_c. \tag{7}$$

The systematic error e_c caused by the sampling, quantization, and centroid algorithm could be calculated by substituting Eqs. (6) and (7) and used for correcting the resolution in the post-processing phase. The resolution of the centroid algorithm is also determined by the noise of the image sensor, which includes three types of noises: the readout noise N_r, the signal photon noise N_p, and the background noise N_b. The background noise and the readout noise impinge all the pixels in the image window; in contrast, the signal photon noise just impacts the pixels illuminated by the laser spot. Since the centroid algorithm processes all the pixels of the image, the centers of both the laser spot and noises are calculated. If the laser spot moves a distance d from x_0, the calculated center $x_d{}'$ is:

$$x_d{}' = \frac{x_r M_{rn} + x_b M_{bn} + x_p M_{pn} + (x_0 + d + e_c)M_s}{M_{rn} + M_{bn} + M_{pn} + M_s}, \tag{8}$$

where x_r, x_b, and x_p are the centers of readout noise, background noise, and light photon noise, respectively, while M_{rn}, M_{bn}, M_{pn}, and M_s respectively represent the mass of readout noise, background noise, light photon noise, and laser spot. As a reference, in a noisy environment, the equation that expresses the original position $x_0{}'$ is listed below:

$$x_0{}' = \frac{x_{r_0} M_{rn} + x_{b_0} M_{bn} + x_{p_0} M_{pn} + x_0 M_s}{M_{rn} + M_{bn} + M_{pn} + M_s}, \tag{9}$$

in which x_{r_0}, x_{b_0}, and x_{p_0} are the original centers of readout noise, background noise, and light photo noise. The background noise and the readout noise follow the Poisson distribution which can be approximately considered as a Gaussian distribution. Since these two noises impact all the image pixels, the center of noises is independent of the laser spot. That is to say, the following relationship holds: $x_{r_0} = x_r$ and $x_{b_0} = x_b$. On the other hand, the signal photon noise is related to the laser spot intensity, thus the assumption could be made that the moved distance of light photon noise approximately equals the moved distance of the laser spot d or $x_p = x_{p_0} + d$. By substituting Eqs. (8) and (9), the systematic error e is shown as:

$$e = \frac{e_c M_s - d(M_{rn} + M_{bn})}{M_{rn} + M_{bn} + M_{pn} + M_s}. \tag{10}$$

The ratio between the calculated distance d' and the moved distance of the laser spot could be expressed as follows:

$$\frac{d'}{d} = 1 + \frac{e}{d} = \frac{M_{pn} + M_s + \frac{e_c}{d} M_s}{M_{rn} + M_{bn} + M_{pn} + M_s}. \tag{11}$$

The systematic error caused by noise can be eliminated or at least reduced in both the capture and post-processing phases. Applying a threshold in the post-processing algorithm can efficiently eliminate the readout noise and background noise. Another post-processing way to reduce noise is to average it using multiple images. If N images are used for the calculation, the noise variance will be dropped to $2/\sqrt{N}$. Temperature also has a very close relationship with the noise. Typically, the CCD temperature should be reduced as much as possible. In the laser deviation measurement system, the temperature increase caused by the laser also increases the noise. In the capture phase, the use of a pulsed laser and synchronized exposure can solve this problem. In Secs. 4 and 5, experiments applying these methods to improve the resolution are described.

For a PSD-based system, the systematic error is mainly due to the amplifier asymmetry for the two current signals I_1 and I_2, ambient light, physical construction of the detector head, and y-axis displacement.[20] Noise is also a key factor that may impact the resolution, including thermal noise current, shot noise, and amplifier noise. To improve the PSD resolution, we can increase interelectrode resistance, which results in a reduction of both amplifier and shot noise. Another way to improve the resolution is to use symmetric and low noise operational amplifiers, but it results in quite an expensive external processing circuit. The error caused by the background light can be eliminated using pulse amplitude modulation, shown in Ref. 6.

3.2 *Speed*

Speed is another important feature for the deviation position measurement. One of the indices to judge PSD speed is response time, defined as the time during which the output signal rises from 10% to 90% of its peak value. The PSD response time depends mainly on the physical features of the PSD, for example its interelectrode resistance and terminal capacitance. Reverse voltage and wavelength of incident light also affect the response time. For most advanced PSDs, the response time can reach 3 μs. In practice, the PSD output signal will be sampled and digitalized for calculation. To reduce the error caused by noise, the average of more than one sample should be calculated. In general, the time cost

for a PSD-based system mainly depends on the sum of the digitalized time and the computing time.

Compared to a PSD, the CCD image sensor cannot output a continuous signal: instead, it generates a series of frames, which is a snapshot of the laser beam spot. The overall processing time t of a separate frame can be approximately calculated as:

$$t = t_e + t_r + t_s + t_l + t_p, \tag{12}$$

in which t_e is the exposure time, t_r is the readout time, t_s is the time used for storing the image, t_l is the image load time, and t_p stands for the algorithm processing time. The readout time includes the time in which all the rows shift into serial register, the time in which the pixels move to the AD converter under clock control, and the time spent by AD conversion and digitization. Exposure time must be long enough for the image sensor capture. The readout time depends critically on the clock frequency, window size, and window position. After the image is generated, the centroid of the algorithm will take time to process the image. Image size, algorithm used, and processor frequency are the main factors impacting the processing time. For an image with $M \times N$ pixels, the time complexity of the centroid algorithm is $O(MN)$.

Several techniques are available to reduce the processing time of image sensors. The CCD with dual serial registers and two amplifiers can speed up the readout time. A laser with larger intensity could shorten the exposure time. The CCD with region of interest and binning features could output fewer pixels, which can also improve the post-processing speed with the cost of lowering the resolution. Implementing the algorithm in hardware is another efficient way to improve the speed of CCD-based systems.

3.3 *Saturation*

Usually, for optical sensors, saturation results in a large error and should definitely be avoided. In practice, the PSD output current follows a good linearity with respect to the laser spot position. If the incident light power is too high and therefore the saturation occurs, the output current is no longer linear with the laser spot position. Hence, the centroid information cannot be retrieved as expected. The parameter "photocurrent saturation" is defined as the total output current when the whole active area of a PSD is illuminated, and is considered to express the saturation performance of the PSD. This value depends on the interelectrode resistance of the PSD and the reverse voltage.[21] A direct way to avoid saturation is to reduce incident light intensity. A PSD with small interelectrode resistance and high reverse voltage can prevent saturation from occurring.

The saturation of the CCD is defined as the maximum amount of charges that the image sensor pixel can collect. This amount of charge a pixel can hold in routine operation is called its full well capacity.[22] One effect of saturation is that the linearity relationship between the number of collected charges and the received light intensity will not stand near the full well capacity, which causes the output signal to generate unexpected distortion. One possible solution to this problem is to adjust the camera gain control so that the full bit depth of the ADC does not span the linear full well capacity of the camera. This makes the image show saturation before real saturation occurs.[23] Another influence is blooming. When the image pixel full well capacity is reached, the more generated charges or the charges that cannot be transferred will pollute the adjacent image areas. A typical phenomenon of blooming is the appearance of a white streak or an erroneous pixel signal value near the high intensity pixels. With respect to measuring the displacement of the laser beams, blooming leads to unexpected and nonrecoverable results, so it should be avoided at all cost. If the camera gain is carefully adjusted to limit the ADC work in the linear full well capacity, blooming will not occur when saturation is just observed. For the application discussed in this paper, the gravity center of a given laser spot is highly related to laser spot intensity, hence, saturation should be avoided in the measurement.

4 Experiment Setup

In Secs. 2 and 3, the factors that might impact the resolution and speed of a CCD-based system, have been described, including the laser beam power, the number of frames used to calculate the position, the image window size, binning, and threshold. To assess the impact of these parameters on system performance, different experiments have been carried out. Since the resolution and speed of PSD-based systems highly depend on the equipment and device themselves, a commercial PSD [Hamamatsu S3932 (Ref. 24)] and external processing circuits [Hamamatsu C3683-01(Ref. 25)] were used in the following experiments for comparing to CCD-based systems.

A diode laser at a wavelength of 635 nm was mounted on a motorized three-dimension micro-positioner with a minimum step size of 0.1 μm, which moved along the x axis of the image under the control of a computer. The laser was directly pointed at a PSD or a DALSA camera,[26] which offers a 1280×960 resolution and a small 3.75×3.75 μm pixel size. In order to control the power of the laser, a polarizer and a filter were set up between the laser and the camera. This setup is shown in Fig. 2. The CCD is removable and can be replaced by a PSD.

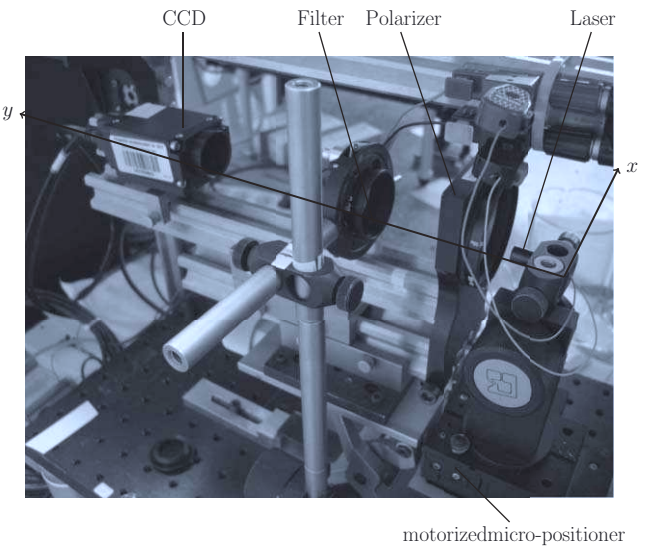

Fig. 2 The experiment setup. The laser is mounted on a motorized micro-positioner, which can move along the *x* direction of the image. The laser is directly pointed at the CCD, which is removable and can be replaced by a PSD.

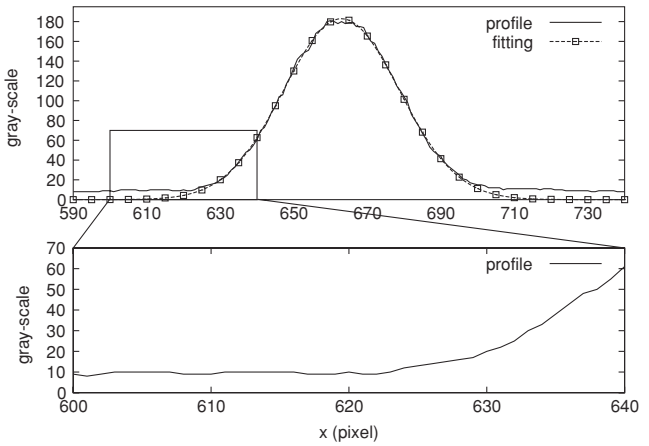

Fig. 3 The upper diagram plots the profile and Gaussian fitting of a laser beam; the lower diagram is the zoom view of the profile between 600 and 640 pixels.

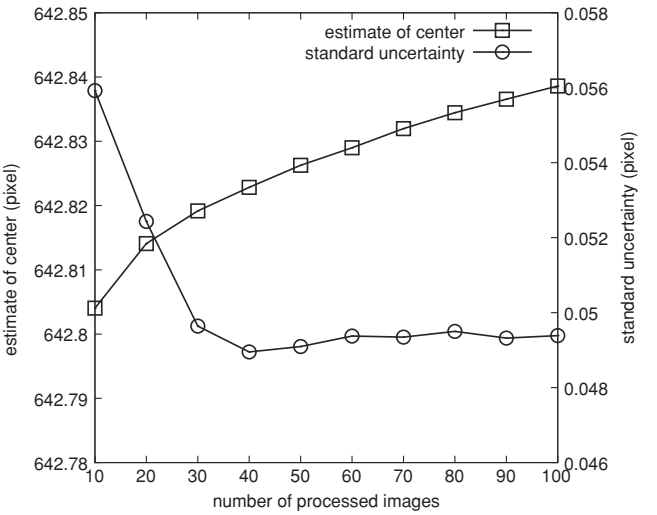

Fig. 4 The estimate of the center and the standard uncertainty of the systematic error against the number of processed images. The curve with squares is the estimate of the calculated center; the curve with circles is the standard uncertainty of the systematic error. The systematic error is assessed by comparing the estimate of the calculated center with the reference center (663.69 pixels). The original point of coordinate is the left bottom corner of the image.

5 Evaluation of parameters

Before comparing the CCD- and PSD-based systems, the factors mentioned in Secs. 2 and 3, should be first considered. An experiment was carried out to analyze these factors. During the experiment, the laser was moved to a specific position and 100 full size images were taken in 4 s. This experiment was repeated 50 times to avoid accidental error. According to these 50 groups of images, different numbers of images were selected in each group and processed with different image window sizes and thresholds. The resolution of the system is assessed from two aspects: systematic error and its uncertainty. For assessing systematic error and its uncertainty, the average of the calculated centers (the estimate of position[27]) and standard deviations (the standard uncertainty[27]) of all the groups were plotted. The power of the laser beam was adjusted to avoid saturation and blooming, as shown in Fig. 3. From the bottom chart in Fig. 3, the gray-scale of the sum of background noise and readout noise reaches about nine. Since the center of the ideal Gaussian spot equals the gravity center of the Gaussian spot, a Gaussian fitting was used to obtain the reference position and the laser beam waist. The average Gaussian center of the images calculated by a Gaussian fitting algorithm in the 50 experiments is 663.69 pixels and the average waist of the laser spot is 15.574 pixels. With different parameters, the estimate of the laser spot position and standard uncertainty were calculated. The systematic error of the CCD-based system was assessed by comparing the estimate of the calculated center with the reference center, whereas the uncertainty was evaluated by the standard deviation of calculated centers. A smaller distance between calculated center and reference center gives a smaller systematic error, and a smaller standard uncertainty is obtained by a smaller standard deviation.

5.1 *Number of Processed Images*

With the 50 groups of images, different numbers of images were selected in each group, and the center of each image was calculated with no threshold and full image size. The estimate of the calculated center and standard uncertainty are depicted in Fig. 4. Both the estimate of center and standard uncertainty in this chart show a trend to stabilize as more images were used. This stability could be attributed to the fact that more images give more noise samples, making the center of noise more stable. The standard uncertainty remains at a level of less than 0.056 pixels, which gives a high level of precision. However, the center given by the experiment is less than 642.9 pixels, which has a large deviation from the reference center 663.69 pixels. According to Eq. (11), the large systematic error is caused by the noises that will lead to the measured distance being much less than the actual distance. Although the result shows a large systematic error, the variance of both estimate of center and standard uncertainty caused by the variance of the processed image number is quite small. That is to say, the resolution of CCD-based systems do not highly depend on the number of processed images. It is a good way to improve speed without greatly reducing resolution.

5.2 *Threshold*

As the number of processed images will not dramatically affect the resolution of a CCD-based system, 10 images were selected for the calculation in the later experiment. As illustrated in Sec. 5.1,, larger noise results in a larger systematic error. Applying a threshold is a common method to eliminate the effect of noises. With different thresholds applied to the full-size images, the estimate of center and standard uncertainty are plotted in Fig. 5. The behavior of estimate and standard uncertainty is quite different between applying a threshold less than the level of noise and applying a threshold larger than the level of noises. When the threshold is less than the level of noise, the systematic error decreased but the standard uncertainty increased as the threshold gets closer to the level of noise. Once the threshold is beyond the level of noise, both the estimate of center and standard uncertainty remain steady and the system reaches high resolution (with estimate of calculated center 663.33 pixels and standard uncertainty 0.045 pixels).

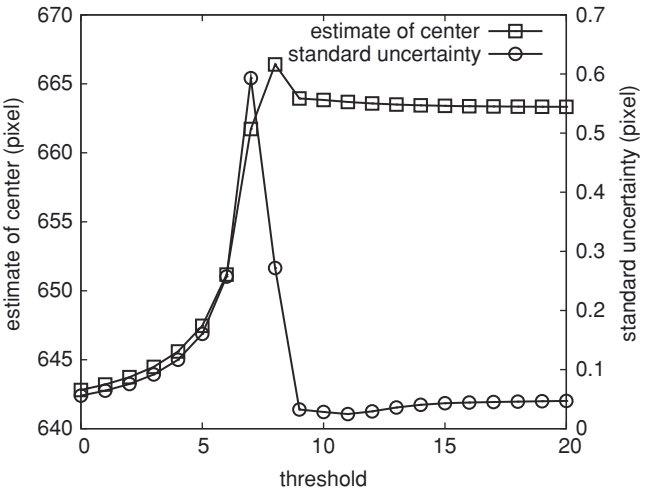

Fig. 5 The estimate of the center and the standard uncertainty of a systematic error against the threshold. The curve with squares is the estimate of the calculated center; the curve with circles indicates the standard uncertainty of a systematic error. The systematic error is assessed by comparing the estimate of the calculated center with the reference center (663.69 pixels). When the threshold is larger than the level of noise 9, both the systematic error and the standard uncertainty are very small. The original point of coordinate is the left bottom corner of the image.

5.3 *Optimum Image Window Size*

Figure 6 describes how image window size affects resolution. The results are calculated with no threshold and 10 images. It is obvious that both the systematic error and uncertainty are sensitive to image window size. As the image window size increased, a smaller uncertainty was obtained, while the systematic error increased. One important reason that might lead to the larger systematic error is the fact that the mass of noises increased as the image window got larger. The effect of the image window size mainly applies to the standard uncertainty, which rises exponentially as the image window decreases linearly. To improve speed by using a smaller image window, the size of the image window should be carefully adjusted according to the performance required from the application.

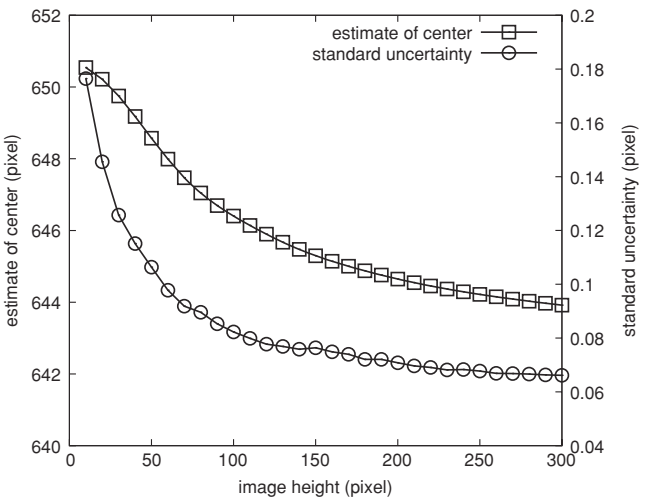

Fig. 6 The estimate of the center and the standard uncertainty of a systematic error against the height of image. The curve with a square is the estimate of the calculated center; the curve with a circle indicates the standard uncertainty of a systematic error. The systematic error is assessed by comparing the estimate of a calculated center with the reference center (663.69 pixels). The original point of the coordinate is the left bottom corner of the image.

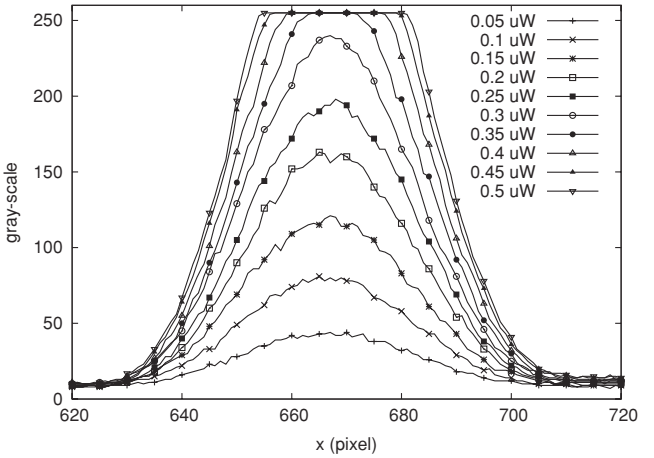

Fig. 7 Profiles of images with different laser beam powers.

5.4 *Laser Beam Power and Saturation*

The power of the laser beam is related to the signal photon noises, which overlay the Gaussian spot. An extremely high laser beam power will lead to saturation or even blooming. All the signal photon noises, saturation, and blooming will interfere with the systematic error and its uncertainty of a CCD-based system. To figure out the systematic error and uncertainty according to different laser beam powers, an experiment was designed and implemented. Figure 7 shows the profiles of images with different laser beam powers, and the estimate of centers and standard uncertainty are plotted in Fig. 8. The curve of the estimate of centers calculated with a

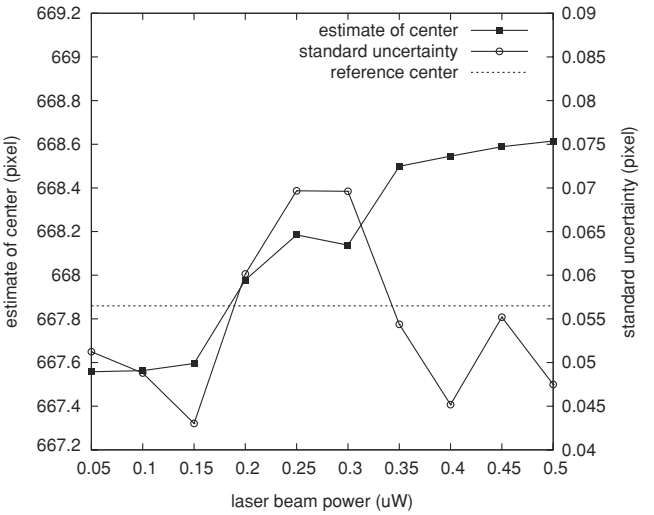

Fig. 8 The estimate of the center and the standard uncertainty of a systematic error against the power of the laser beam. The curve with squares is the estimate of the calculated center; the curve with circles is the standard uncertainty of a systematic error. The systematic error is assessed by comparing the estimate of a calculated center with the reference center. The dashed line indicates the reference center calculated by Gaussian fitting. The original point of coordinate is the left bottom corner of the image.

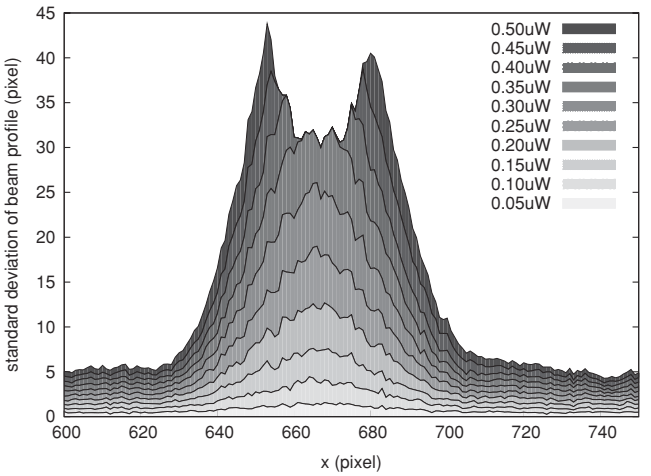

Fig. 9 The standard deviation of the laser beam profile in different powers, shown in different gray-scales.

different laser power turns out to be a transformation between two states. One state happens when the laser power is less than 0.15 μW, while another occurs after a laser power larger than 0.35 μW. Between these two states, the estimate of center increases quickly as the laser power increases. The slight decrease of 0.3 μW is possibly caused by accidental error. The formation of the first state is due to the low noises brought by the low laser power, which can be observed in Fig. 9. The low standard uncertainty at the same phase further proves this explanation. These noises affect the systematic error in this state, which shows a difference between the reference center (obtained by Gaussian fitting to the images with different powers, 667.86 pixels) and the calculated center. With the increase in laser power, both the standard uncertainty and the estimate of center increased quickly. This trend continues until saturation occurs at the power of 0.35 μW, as shown in Fig. 7. From Fig. 9, it is clear that the noise rises with the increase of laser power. This impacts the standard uncertainty of the systematic error so that it gives a larger uncertainty when the laser power increases. In addition to noise impacting the systematic error, another factor that affects the systematic error is the fact that the laser polarization might not be ideally uniform. This makes the Gaussian spot center move toward one direction when adjusting the power by polarizer. Compared with Figs. 7 and 8, it is obvious that the second state is due to saturation, which hides most of the signals and noises at the top of the laser spot intensity. Since the noises are hidden by saturation, the standard uncertainty reduced to the level of the first state. Both low laser power and saturation provide the system a small uncertainty and a large systematic error. To obtain a smaller systematic error, the power of the laser should be adjusted appropriately to avoid a low signal-to-noise ratio and saturation.

6 Comparison

To compare the two different methods, the CCD image window size was cut to be the same size of the PSD, that is 4.8×1 mm (1280×267pixels). The response of the two methods to various factors was taken by moving the motorized micro-positioner with a step of 0.1μm, which is considered to be the reference measure to compare the two methods. During each step, 10,000 samples of PSD signals and 64 images were captured in 1 second. For PSD, the laser beam position was calculated by averaging the 10,000 PSD signal samples, while the average image of 65 images was used to compute the laser beam position by the centroid algorithm with threshold 10 applied. To obtain a full-range comparison, five zones that are oriented from the center of the sensor were chosen to perform the measurement. In each zone, the micro-positioner was moved by 50 steps. To guarantee that a complete laser beam is contained in the active sensor surface, the range of the measurement is set to the range of -1 to $+1$ mm according to the laser beam waist (46.6 pixels in this experiment). The laser was synchronized with the camera exposure by a National Instrument DAQ card in pulse mode. The CCD saturation is avoided by applying a polarizer to reduce the laser power and setting the exposure time to 13 μs. All the experiments are carried out in a dark room to obtain the best performance.

Table 1 The slopes for different zones with CCD and PSD.

	0 mm	$+0.5$ mm	$+1$ mm
CCD (pixel/μm)	0.2622	0.2462	0.2625
PSD (V/μm)	0.0019	0.0018	0.0017

6.1 *Resolution*

For comparing the resolution of both methods, these centers for PSD, and CCD-based systems with different units were converted to distance. The slope of the best fit line indicates the ratio between the measurement unit and the distance. Thus the slopes are used to convert the measurement units to distances which are listed in Table 1. In this table, the slopes for a CCD-based system are very close to the inverse of the image pixel size (0.267 pixel/μm), which shows that the systematic error of the CCD-based system is very small according to Eq. (11). The uncertainty of the systematic error can be evaluated by the standard deviation of the error according to the best fit line. The estimate of calculated centers and the error according to the best fit line of both a CCD and a PSD in each measurement zone are depicted by Fig. 10, which shows good linearity for all the zones. The chart in the second row of Fig. 10 shows that the error of the PSD-based system is larger than that of the CCD-based system. The standard uncertainty of the errors in each zone are plotted in Fig. 11, from which we can observe that the uncertainty of the PSD-based system will gradually increase as the laser beam leaves the center. In contrast, the CCD-based system presents a good consistency in all the positions, with an average standard uncertainty ±0.068 μm. It is obvious that the uncertainty of the CCD-based system is much less than the uncertainty of the PSD-based system (average standard uncertainty ±0.1077 μm) under the same operating conditions. And the resolution of the CCD-based system is insensitive to the laser spot position compared to the PSD-based system.

6.2 *Speed*

During the experiment, the duration of both capture and processing was recorded simultaneously. The program was implemented in C and was carried out in a DELL notebook LATITUDE E6500. For the PSD-based system, the duration

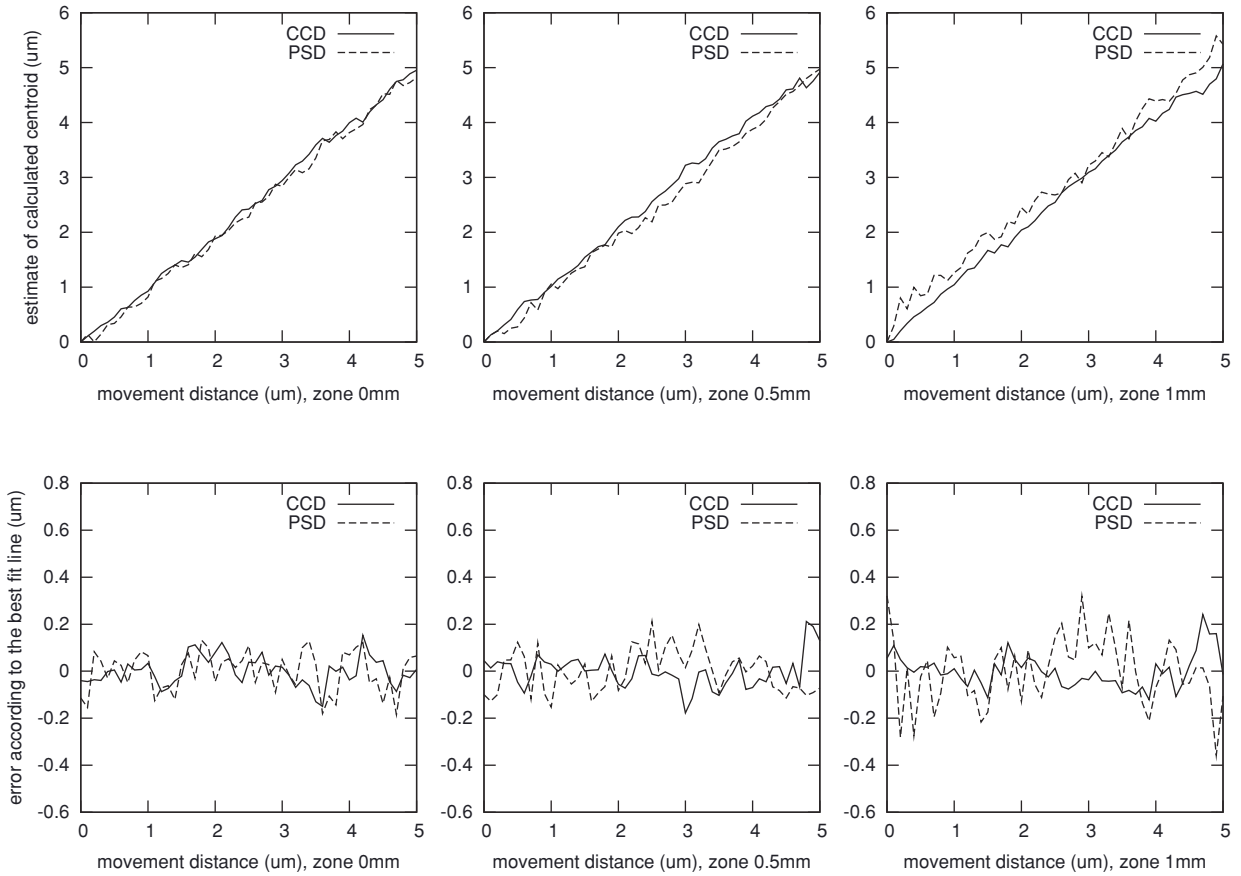

Fig. 10 The estimate of the center and the error according to the best fit line against the distance moved. The first row shows the estimate of the calculated centroid for a CCD and a PSD. The second row shows the error for a CCD and a PSD according to the best fit line. From left to right, the position of 0 mm, the position of $+0.5$ mm, and the position of $+1$ mm.

contains not only the time used for capturing, sampling, and digitalizing, but also the time elapsed for calculating the average. In addition to these, the image store and load time are also considered for the CCD-based system. Figure 12 shows the time cost to obtain one laser beam position for both of the systems. The time cost by PSD processing is very short, with an average of 0.35 ms. The primary time cost of the PSD-based system is capture, which highly depends on the sample rate of the external circuit. Compared with the stability of the time cost associated with the PSD-based system, the time cost of the CCD-based system depends greatly on the storage access time (store and load), which takes 80.4% of the total time on average due to the low speed of the

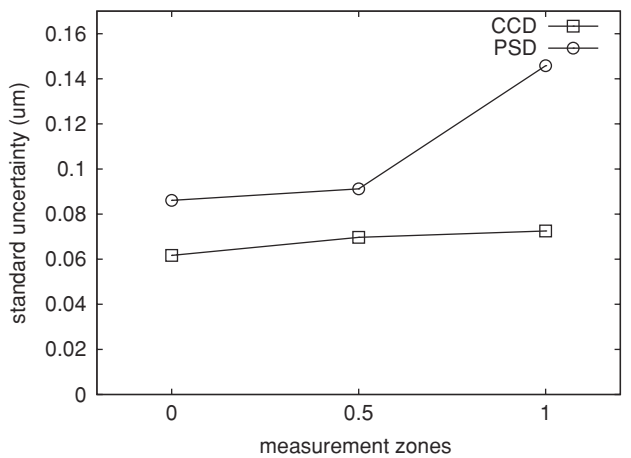

Fig. 11 The standard uncertainty of a systematic error. The first row shows the result with a CCD, the second row shows the result of a PSD. The systematic error is assessed by comparing the estimate of the calculated center with the best fit line. From left to right, the position of 0 mm, the position of $+0.5$ mm, and the position of $+1$ mm.

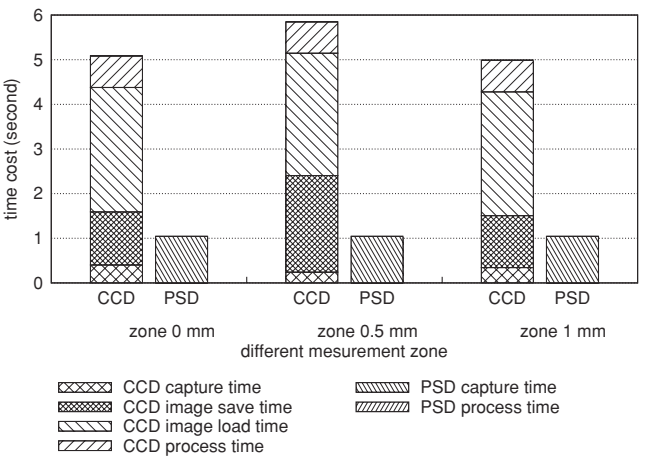

Fig. 12 Time cost in both a CCD-based system and a PSD-based system.

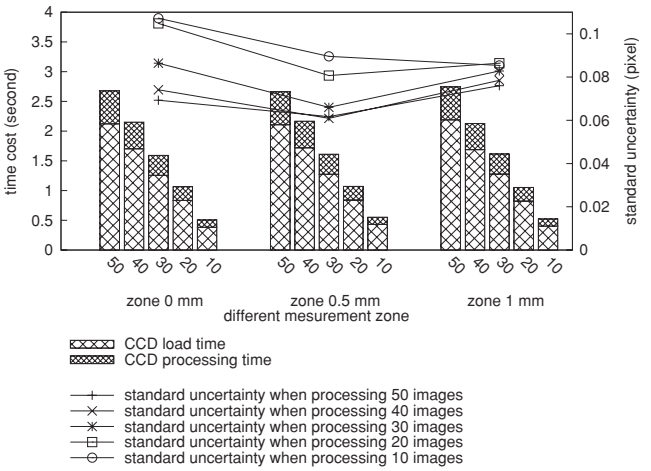

Fig. 13 Uncertainty and time cost for processing different numbers of images. The bars in the graph indicate the time cost with different numbers of processed images in different zones. The lines present the standard uncertainty of the systematic error with different numbers of processed images in different zones.

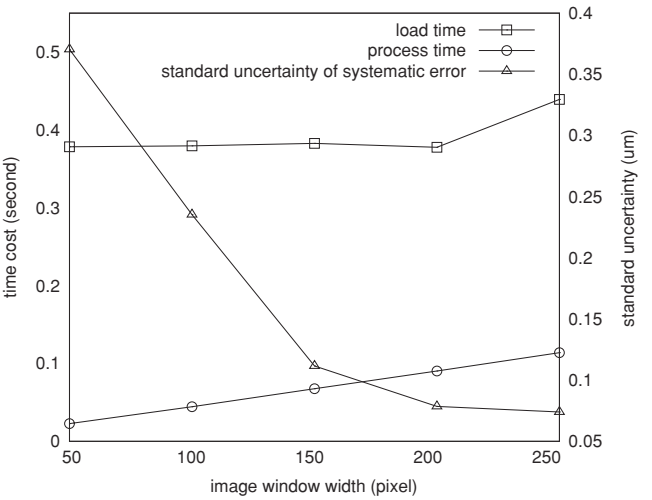

Fig. 14 Uncertainty and time cost for processing different image windows in position 0 mm. The curve with squares is the time cost on loading the image for different image window widths. The curve with circles represents the process time for different image window widths. The curve with triangles indicates the standard uncertainty of the systematic error according to the image window width.

storage device. A possible improvement is to store all the images in memory, which is much faster than the external storage device. Furthermore, the processing time will also be reduced due to the fast readout speed of memory. Although the actual processing time reaches about 0.7 s on average, which is much longer than the PSD-based system, it only takes 13% of the total time. The time cost on capture and processing is 1.036 s, which nearly equals the time cost of a PSD-based system (1.044 s). Thus, the critical time cost by a CCD-based system is the storage access time, which needs to be optimized in the system design and implementation.

6.3 *Performance Trade-Off of CCD-Based System*

6.3.1 *Number of images processed*

As discussed in Sec. 3.2, the time complexity of processing K images with the size of $M \times N$ is $O(KMN)$. The time cost by image processing is related to both the number of images and the image size. In previous experiments, 65 images were used to calculate the center of a laser beam. With the same image set, different numbers of images were selected and used to calculate the center. The standard uncertainty of systematic errors and time costs for this processing are shown in Fig. 13. Time cost is a position-insensitive quantity, which decreases linearly as the number of processed images is reduced. With the decrease of processed images, the calculated centers indicate a tendency toward growth. When 10 images were used for the centroid calculation, the time cost by loading and processing images decreased to 0.53 s on average and the standard uncertainty of error rise to $\pm 0.094\ \mu$m, which increased by 36.2% compared with the standard uncertainty of error of processing 50 images (average standard uncertainty of error is $0.069\ \mu$m). However, this uncertainty is still smaller than the uncertainty of the PSD-based system mentioned in Sec. block block. Although fewer images are processed, the uncertainty of the systematic error will increase, and the number of processed images will not greatly reduce the resolution. In practical applications, reducing the number of images is a good way to improve speed without losing much resolution.

6.3.2 *Image window*

Another way to reduce the processing time is to diminish the image size. To maintain the measurement range, the length of the image window remained at 4.6 mm (1280 pixels) and the width of the image window was diminished from 267 pixels to 250, 200, 150, 100, and 50 pixels. The same image set was used but preprocessed by an image window algorithm, which generates the desired image size. According to the Sec. 6.3.1, 10 images were used for calculating the position of the laser beam to obtain the worst resolution. The uncertainty of the systematic error and time cost are depicted in Fig. 14. As the image width decreased, the uncertainty of the systematic error rose very quickly, from $0.074\ \mu$m to $0.37\ \mu$m. Compared with the speed improvement gained by reducing the number of processed images, a smaller image window did not improve the speed remarkably. There is only a benefit of 0.152 s in speed (load time and processing time), with an increase of $0.3\ \mu$m standard uncertainty. As the image width decreases, the time cost decreases linearly, while the uncertainty of the systematic error increases exponentially. This shows a clear constraint for a CCD-based system: the image window width should be larger than the size of the laser spot; otherwise, the resolution will decrease exponentially as the image window width decreases.

6.3.3 *Binning*

Binning is the process of combining charges from adjacent pixels in a CCD during the readout phase. It will improve the readout speed at the expense of reducing the image dimension in pixels (number of image pixels). Since the charge of adjacent pixels will be read out at the same time, the read out noise of the CCD working in binning mode will decrease compared to the CCD working in non-binning mode. However, the background noise will increase due to a larger exposure area per pixel unit. An experiment of binning was carried out under the same environment as the previous experiments. A 2×2 binning was applied for the measurement, thus image dimension reduced to 640×133 pixels. To verify the effect

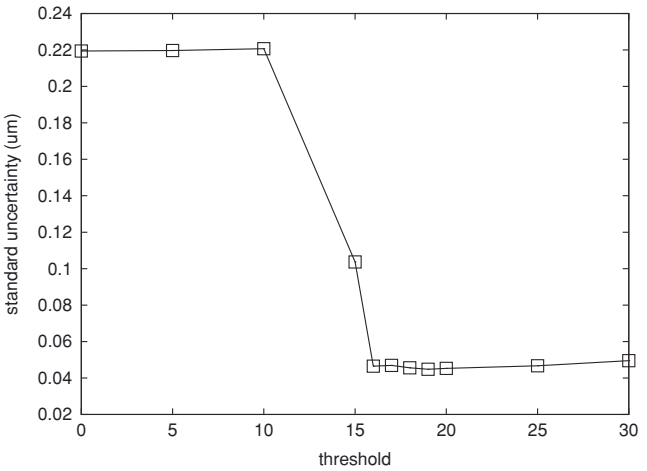

Fig. 15 Standard uncertainty of the systematic error for different thresholds. Binning will cause the level of noise increase when the background illumination is high. Applying a higher threshold can improve the resolution when using the binning technique.

of the noise, different thresholds were applied to 10 images for each position. The standard uncertainty of the systematic error are plotted in Fig. 15. The threshold 10, which was applied for the previous experiments, is not effective enough in the case of 2×2 binning. The standard uncertainty of the systematic error ($\pm 0.2423\,\mu$m) for applying threshold 10 is nearly the same as the one without applying the threshold ($\pm 0.2469\,\mu$m). However, with a threshold of 19, the standard uncertainty reduced to the minimum value $\pm 0.0448\,\mu m$, after which the standard uncertainty of the systematic error increased slightly as the threshold increased. Until applying the threshold of 85, the standard uncertainty remained at a level of less than 0.1 μm. The average load time and process time reduced to 0.3 and 0.1 s separately. Binning will lead to a fast system speed with more noise when the background illumination is high. Under a high illumination situation, the binning technique should be used with a higher threshold to maintain high resolution.

7 Conclusion

Both the PSD and the CCD provide the capability of measuring laser beam deviations. As an analogue device, the PSD simply outputs two photocurrents to represent incident light position. The CCD utilizes a series of pixels which form a 2D image window to record the incident light intensity distribution. This 2D image window provides more information for post-processing. A narrow image window loses a lot of information, while a wide image window brings more noise and computation load. The optimal image window can be decided by the performance requirement of the application. In this paper, measurement achieved in a clear medium in a lab environment shows that the average resolution of a CCD-based system is nearly 1.5 times the average resolution of a PSD-based system. Furthermore, the resolution of a CCD-based system is independent of the incident laser beam position, while the PSD-based system obtains worse resolution as the laser beam position gets farther from the center of the PSD.

The performance of a CCD-based system could be adjusted by adjusting different parameters. A small image window size is useful not only for increasing the resolution but also for improving the speed with the limitation that the laser spot should be entirely contained in the image. Applying a threshold to the noise level could efficiently reduce the systematic error. To improve the speed, binning is an alternative means, but the noise level should be reconsidered to choose a proper threshold. Saturation hides a lot of the laser spot information and thus should be definitely avoided. According to the analysis and experiment results provided in this paper, a CCD-based system can obtain better resolution than a PSD-based system with a comparable speed to a PSD-based system by adjusting these parameters. This makes the CCD a better alternative to the PSD in beam deviation measurement applications. Furthermore, the CCD records all the power distribution information of the laser spot, thus giving the capability of measuring the power distribution sensitive quantities, such as the turbidity of seawater.

1. D. Malardé, Z. Y. Wu, P. Grosso, J.-L. de Bougrenet de la Tocnaye, and M. Le Menn, "High-resolution and compact refractormeter for salinity measurements," *Meas. Sc. Technol.* **1**, 20 (2009). Q10
2. H. Canabal, J. Alonso, and E. Bernabeu, "Laser beam deflectometry based on a subpixel resolution algorithm," *Opt. Eng.* **40**, 2517 (2001).
3. J. T. Wallmark, "A new semiconductor photocell using lateral photoeffect," *Proceedings of the Institute of Radio Engineers*, Vol. **45**, pp. 474–483 (1957). Q11
4. H. X. Song, X. D. Wang, L. Q. Ma, M. Z. Cai, and T. Z. Cao, "Design and performance analysis of laser displacement sensor based on position sensitive detector (PSD)," *J. Phys.* **48**(1), 217–222 (2006).
5. Z. Huili, H. Xiaorui, Z. Yuning, and W. Xuanze, "Research on position detection of psd based on light intensity modulation and digital fit," *Int. J. Intell. Syst.* **3**, 38–42 (2009).
6. W. Guanghui, P. Shum, X. Guoliang, Z. Xuping, "Position detection improvement of position sensitive detector (psd) by using analog and digital signal processing," *2007 6th International Conference on Information, Communications & Signal Processing*, pp. 1–4 (2007).
7. G. Philippe, M. Damien, M. Le Menn, W. Zongyan, and J.-L. de Bougrenet de La Tocnaye, "Refractometer resolution limits for measuring seawater refractive index," *Opt. Eng.* **49**(10) (2010). Q12
8. P. F. I. Scott, A. S. Kachatkou, N. R. Kyele, and R. G. van Silfhout, "Real-time photon beam localization methods using high-resolution imagers and parallel processing using a reconfigurable system," *Opt. Eng.* **48**, (2009). Q13
9. S. S. Welch, "Effects of window size and shape on accuracy of subpixel centroid estimation of target images," NASA Technical Paper 3331, September 1993.
10. N. Bobroff, "Position measurement with a resolution and noiselimited instrument," *Rev. Sci. Instrum.* **57**, 1152–1157 (1986).
11. M. R. Shortis, T. A. Clarke, and T. Short, "A comparison of some techniques for the subpixel location of discrete target images," *Proc. SPIE* **2350**, 239–250 (1994).
12. T. A. Clarke and X. Wang, "Analysis of subpixel target location accuracy using Fourier-transform-based models," *Proc. SPIE* **2598**, 77–88 (1995).
13. R. Singh, J. M. Hattuniemi, and A. J. Mäkynen, "Analysis of accuracy of the laser spot centroid estimation," *Proc. SPIE* **7022** (2007). Q14
14. B. F. Alexander and K. C. Ng, "Elimination of the systematic error in subpixel accuracy," *Opt. Eng.* **30**, 1320–1331 (1991).
15. H. Chen and C. Rao, "Accuracy analysis on centroid estimation algorithm limited by photo noise for point object," *Opt. Comm.* **282**(8), 1526–1530 (2009).
16. T. A. Clarke, M. A. R. Cooper, and J. G. Fryer, "An estimator for the random error in subpixel target location and its use in the bundle adjustment," *Proc. SPIE* **2252**, 161–168 (1994).
17. J. W. Cui, J. B. Tan, L. Ao, and W. J. Kang, "Optimized algorithm of the laser spot center location in strong noise," *J. Phys.: Conf. Ser.* **13**, 312–315 (2005).
18. I. Edwards, "Using photodetectors for position sensing," Sensors Magazine, Dec. 1988.
19. Bracewell and R. Newbold, *The Fourier Transform and its Applications*, McGraw-Hill, New York (1978). Q15
20. S. Iqbal, M. M. S. Gualini, and A. Asundi, "Measurement accuracy of lateral-effect position-sensitive devices in presence of stray illumination noise," *Sens. Actuators, A* **143**, 286–292 (2008).
21. HAMAMATSU PHOTONICS K.K., Solid State Division, Characteristics and use of psd. http://sales.hamamatsu.com/assets/pdf/catsandguides/psd_technical_information.pdf.

Q16
22. S. B. Howell, *Handbook of CCD Astronomy*, Cambridge University Press (2000).
23. HAMAMATSU PHOTONICS K.K., Solid State Division. Ccd saturation and blooming. http://learn.hamamatsu.com/articles/ ccdsatandblooming.html.
24. HAMAMATSU PHOTONICS K.K., Solid State Division. One-dimensional psd s3931, s3932, s3270. http://sales.hamamatsu.com/assets/pdf/parts_S/s3931_etc_kspd1002e05.pdf.
25. HAMAMATSU PHOTONICS K.K., Solid State Division. Signal processing circuit for 1D psd c3683-01. http://sales.hamamatsu.com/assets/pdf/parts_C/C3683-01.pdf.
26. DALSA Corporation. Genie m1280 datasheet, 2009. http://www.dalsa.com/prot/mv/datasheets/genie_m1280_1.3.pdf.
27. BIPM, IEC, IFCC, ISO, IUPAC, IUPAP, and OIML, "Guide to the expression of uncertainty in measurement," ISO, Geneva, 1993.

Bo Hou is a PhD student at Telecom Bretagne, France. He received his MS degree in computer science from Beijing University of Posts and Telecommunications. He has worked for IBM China Development Laboratory, researching and developing Business Intelligence systems. His research interests include information systems, image processing, and high-precision instrumentation.

Biographies and photographs of the other authors not available.

Queries

Q1: Au: Please supply authors first names.
Q2: Au: Please check the placements of Ref. 18.
Q3: Au: Please check placement of Ref. 19.
Q4: Au: Please define AD.
Q5: Au: Please check change from “the previous section” to “Secs. 2 and 3”.
Q6: Au: Please check change from “the previous section” to “Secs. 2 and 3”.
Q7: Au: Please check change from “the previous section” to “Sec. 5.1”.
Q8: Au: Please indicate to which section you are refering to in “last section”.
Q9: Au: Please check change from “last section” to “Sec. 6.3.1”.
Q10: Au: Please supply page range for Refs. 1, 2, 8.
Q11: Au: Please provide publisher/sponsor and location for Refs. 3 and 6
Q12: Au: Please check author names in Ref. 7 and supply page range.
Q13: Au: Please check Ref. 7 for content errors, or provide the DOI.
Q14: Au: Please supply volume or page range for Ref. 13
Q15: Au: Please supply initial of 1st author in Ref. 19.
Q16: Au: Please supply location of publisher in Ref. 22.